The Microstrains Observed in the Walls of Large Tubes under Internal Pressures up to 6 kbar

L. Deffet and J. Gouzou

INTRODUCTION

The study of the behaviour of thick-walled cylinders was initiated in 1960 by the Institut Belge des Hautes Pressions (IBHP). Previous tests had shown that a size effect existed at the onset of plastic strain and fracture of geometrically similar cylinders, i.e. of cylinders having the same outer diameter/inner diameter and length/diameter ratios, but different wall thicknesses (1)–(3)*. This size effect resides in the fact that small cylinders possess a better resistance to the progressive application of an internal pressure: they strain plastically and fracture at higher pressures than large cylinders. The relationships established by Lamé do not account for this difference: according to them, geometrically similar cylinders should strain plastically at a given pressure and burst at another pressure, both pressures being independent of the cylinder size.

This size effect was studied more thoroughly, from 1962, by IBHP and the Centre National de Recherches Métallurgiques (CNRM) working in close co-operation. The first results obtained showed that anelastic strains were observed in thick-walled cylinders earlier than generally thought, and led to a better knowledge of the stress distribution in these cylinders (4).

The present work was aimed at (1) checking whether or not thick-walled cylinders made from various steels exhibit a size effect at the onset of plastic strain, and (2) acquiring a better understanding of the phenomena which precede the onset of plastic strain in a thick-walled cylinder subjected to an internal pressure, in order to be in a position to calculate the complete stress distribution in such a cylinder.

STEELS USED IN THE TESTS

Four steels were used to manufacture the cylinders:

(A) a low-carbon steel;
(B) a medium-carbon steel;
(C) a quenched-and-tempered steel;
(D) an austenitic stainless steel.

The chemical composition and mechanical properties of these steels are listed in Table 1.

* *References are given in Appendix 2.*

TESTING

A comparison was made of the behaviour of geometrically similar cylinders with an outer diameter/inner diameter ratio of 2, and wall thicknesses ranging from 5 to 50 mm. These cylinders were subjected at room temperature to a progressively increasing internal pressure, and the following parameters were determined for each cylinder:

(1) the pressure corresponding to the onset of plastic strain;
(2) the strains present at the outer surface of the cylinder as the pressure is raised from zero to its maximum value.

The following rules were observed in order to obtain the best possible reproducibility:

(1) All the cylinders in a given series were manufactured from the same steel, in order to avoid any variation in the properties of material from one cylinder to the next.
(2) The length of each cylinder was approximately four times its outer diameter.
(3) Great care was taken to raise the pressure in all the cylinders of a series according to a strictly identical law, in order to ensure that the strain rate did not vary from one cylinder to the next.
(4) Pressures were measured by means of a free-piston gauge, with an accuracy of $0{\cdot}5 \times 10^{-3}$.
(5) The strains at the surface of the cylinders were measured by means of strain gauges with a sensitivity of 10^{-6}, the equipment used being capable of measuring the strains at 10 locations on each cylinder.

SIZE EFFECT

The test results confirm the existence of a size effect for steels A, B, and C: when geometrically similar cylinders made from the same steel are compared, it is seen that the pressure corresponding to the onset of plastic strain decreases slightly as the cylinder's size is increased.

In order to explain this size effect, the influence of microscopic material defects on the onset of plastic strain will be examined. As is known, the fracture strength of brittle materials has been tentatively attributed to the existence of defects or microcracks. Such microscopic

Table 1

Steel	Chemical composition, wt %							Mechanical properties, MN/m²	
	C	Mn	Si	Cr	Mo	Ni	Cu	Yield stress	Ultimate tensile strength
A	0·10	0·50	0·19	—	—	—	—	233	416
B	0·31	0·55	0·31	—	—	—	—	325	532
C	0·37	0·59	0·34	1·63	0·28	1·53	—	1076	1193
D	0·05	1·30	0·40	26·0	2·50	8·50	1·51	672	922

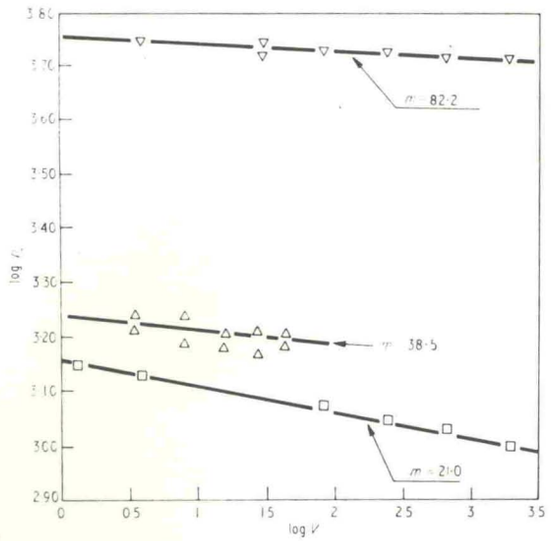

□ Steel A.
△ Steel B.
▽ Steel C.

Fig. 1. Variation of p_e as a function of cylinder size

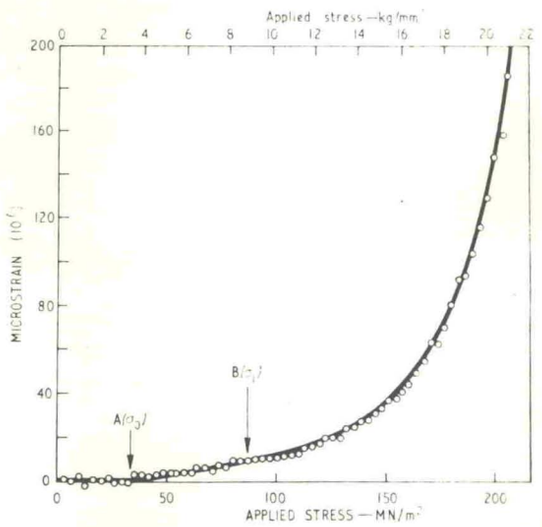

Fig. 2. Microplasticity curve for steel A at +20°C

defects are naturally more numerous in a large part, and their presence accounts for the existence of a size effect as regards fracture. Weibull (5) has evolved a statistical theory of the strength of materials which is based on this explanation.

It appears reasonable to assume that Weibull's statistical theory also holds in the case of plastic strain. Richards has used this concept to explain the size effect relating to the upper yield stress of mild steel, both in tension (6) and in bending (7). In the case of plastic strain, the microscopic defects in the material would no longer be microcracks but very small regions in which plastic strain is very easy—for instance, small regions containing dislocation sources.

Assuming that the statistical theory put forward by Weibull applies to plastic strain in thick-walled cylinders, the pressure, p_e, corresponding to the onset of plastic strain, must decrease as the size increases according to the law:

$$p_e = \frac{p_{e1}}{V^{1/m}} \quad . \quad . \quad . \quad . \quad (1)$$

where p_{e1} is the pressure for the onset of plastic strain in a cylinder of unit volume, V is the volume of the cylinder considered, and m is a constant for a given material. In Fig. 1, in which $\log p_e$ has been plotted versus $\log V$, the volume of the smallest cylinder has been selected as the unit volume. This figure shows that a size effect actually exists, and that the experimental results fit in satisfactorily with Weibull's theory. It is seen that the exponent m increases with increasing yield stress of the material, which means that the size effect is sharper in a mild steel than it is in a high-strength steel.

CALCULATION OF THE STRESS DISTRIBUTION IN A THICK-WALLED CYLINDER

In order to understand better the phenomena which precede the onset of plastic strain in a thick-walled cylinder, and to be in a position to calculate the complete stress distribution in such a cylinder, the plastic properties of the material must be known as fully as possible. In this respect, three important aspects have to be discussed: (1) the microplasticity of the steel, (2) the criterion of yielding, and (3) the general relation between stress and plastic strain.

Microplasticity of the steel

When discussing the mechanical behaviour of a steel in terms of the conventional tensile test, it is generally assumed that the upper yield stress constitutes a natural limit below which the metal strains elastically, and above which it strains plastically. A detailed investigation of the phenomenon shows that the conventional tensile test does not provide a full description of the mechanical properties. In actual fact there is a transition between the elastic and plastic fields which can be studied more thoroughly through microplasticity measurements.

In order to determine the microplasticity curve of a material, use is made of a deadweight tensile testing machine in which the applied stress is increased according to a linear law ($d\sigma/dt$ = constant). The test is carried out at a carefully controlled temperature ($\pm 0{\cdot}02$ degC), and the elongations are measured by means of a high-sensitivity extensometer ($\pm 1 \times 10^{-6}$) which is photographed at regular time intervals during the test (8).

Fig. 2 shows the microplasticity curve of steel A. This curve was recorded at a temperature of +20°C, using a loading rate of $7{\cdot}6 \times 10^{-3}$ kg/mm² s. At the start of the test, i.e. below point A corresponding to a given threshold value, σ_0, no microstrains are observed, and the strains are thus purely elastic. At this moment the dislocation density is of the order of 10^8 cm/cm³; in other words, the dislocations are too few to give rise to a measurable plastic strain. Between A and B, where B corresponds to a second threshold value, σ_1, microstrains are observed which increase according to a linear law. They can be attributed to small movements of the dislocations existing in the steel, without any formation of additional dislocations (9). At point B, the dislocation sources come into play, and progressively increase the dislocation density up to a value of the order of 10^{10}–10^{11} cm/cm³, at which level macroscopic plastic strain sets in. This part of the test is characterized by a parabolic law of microstraining:

the parabola is of the second order as long as the microstrains do not exceed 10^{-5}, and progressively transforms into a higher order parabola (**10**). During this part of the test a low increase in the applied load leads to a sharp increase in strain.

The microstrain measurements show that plastic strain sets in progressively. The concept of a material which remains perfectly elastic up to a certain critical stress, beyond which plastic strain sets in abruptly, must therefore be rejected. Strictly speaking, the 'yield point' does not exist.

The microplasticity curve of Fig. 2 can be described by the following equation:

$$\epsilon_p = C_0(\sigma-\sigma_0)+\frac{C_1C_2(\sigma-\sigma_1)^n}{[1-C_1(\sigma-\sigma_1)][1-2C_1(\sigma-\sigma_1)]} \quad (2)$$

where ϵ_p is the microstrain, σ the applied stress, and C_0, C_1 and C_2 depend on the composition and structural condition of the material. In most cases the exponent n is equal to 2, although it can have other values for certain materials. This form of the law of microplasticity is not that supplied by the structural study of the phenomenon (**8**), but that which fits in best with the experimental data for a large number of materials. The first term in equation (2) exists only if $\sigma \geqslant \sigma_0$, and the second only if $\sigma \geqslant \sigma_1$.

Criterion of yielding

The Maxwell–von Mises criterion is known to be that which describes most accurately the onset of plastic strain in a steel subjected to combined stresses. It has recently been shown (**11**) that this criterion derives directly from Eyring's thermodynamic model (**12**), provided that plastic strain under combined stresses is assumed to result from a simple superimposition of plastic shear strains in planes making an angle of 45° with the directions of the principal stresses, each shear strain depending solely on the shear stress in the corresponding plane.

As a mater of fact, if plastic strain is due to a thermally activated movement of dislocations, the shear strain rate, $\dot{\gamma}$, is given by an equation of the type

$$\dot{\gamma} = 2A \exp\left(-\frac{W}{kT}\right) \sinh\left(\frac{V\tau}{kT}\right) \quad . \quad . \quad (3)$$

where k is Boltzmann's constant, T the absolute temperature, τ the shear stress applied to the dislocation, V the activation volume, W the activation energy, and A is a constant which embodies several structural factors. Granting the simple superimposition of plastic shear strains in planes lying at 45° to the principal stresses, the largest strain rate is found in the direction of the highest principal stress, and is equal to

$$\dot{\epsilon}_1 = 2A \exp\left(-\frac{W}{kT}\right)\left[\sinh\frac{V(\sigma_1-\sigma_3)}{2kT}+\sinh\frac{V(\sigma_1-\sigma_2)}{2kT}\right] \quad . \quad . \quad . \quad (4)$$

Assuming that the yield stress corresponds to the stress level at which $\dot{\epsilon}_1$ reaches and exceeds a certain critical threshold value, it is possible to derive the yield stress corresponding to any system of stresses. This calculation has been made in the case of stress systems comprised between pure tension and pure shear stress. The theoretical law thus obtained is shown in Fig. 3, where σ/σ_y has been plotted against τ/σ_y, as is often done for these stresses. This figure also contains the Maxwell–von Mises

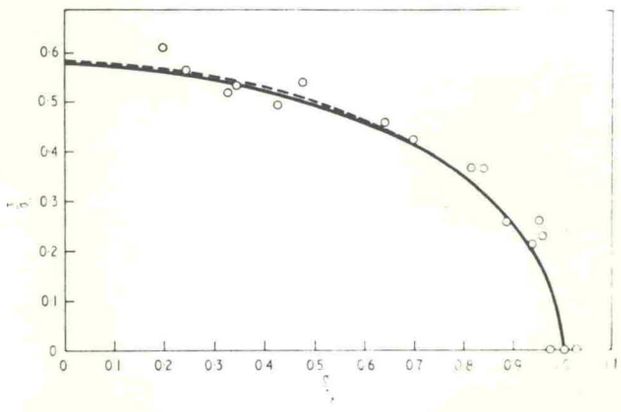

— — — Maxwell–von Mises criterion.
——— Law derived from equation (4).
○ Experimental data.

Fig. 3. Plasticity threshold for a mild steel at room temperature according to reference (11)

relation, and a set of experimental points determined at room temperature. It is seen that the theoretical law derived from equation (4) is almost identical with the Maxwell–von Mises relation.

In order to calculate the onset of plastic strain in a steel subjected to combined stresses, it can thus be assumed that the strain results from a simple superimposition of plastic shear strains in planes lying at 45° to the principal stresses: this mode of calculation leads to practically the same results as the Maxwell–von Mises relation.

General relation between stress and plastic strain

The most frequently used strain law is the Lévy–von Mises relation, which assumes that the plastic shear strains in planes lying at 45° to the principal stresses are proportional to the shear stresses in these planes. It is known that stresses and strains can be characterized by two dimensionless parameters, μ and ν which have been proposed by Lode (**13**):

$$\mu = \frac{2\sigma_2-\sigma_1-\sigma_3}{\sigma_1-\sigma_3}; \qquad \nu = \frac{2\Delta\epsilon_2-\Delta\epsilon_1-\Delta\epsilon_3}{\Delta\epsilon_1-\Delta\epsilon_3} \quad (5)$$

and that the use of the Lévy–von Mises relation implies $\nu = \mu$. Since this equality is not confirmed experimentally, it must be concluded that the Lévy–von Mises relation does not give a satisfactory description of plastic strain under combined stresses (Fig. 4).

On the contrary, if it is assumed that plastic shear strains are proportional to the strain rates in the planes lying at 45° to the principal stresses, i.e. that the principal plastic strains can be derived from three equations similar to equation (4), another strain law is obtained. Fig. 4 shows that this law accounts satisfactorily for the experimental results (**11**).

Therefore, the model of plastic strain set out above, which involves the simple superimposition of plastic shear strains in planes lying at 45° to the principal stresses, provides a suitable explanation for both the onset of plastic strain in a material and the law of plastic strain under combined stresses. Hence, this model can replace both the Maxwell–von Mises criterion and the Lévy–von Mises strain law.

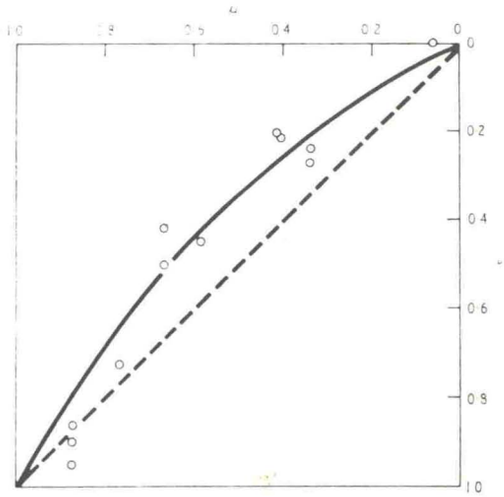

— — — Lévy–von Mises relation.
——— Law derived from equation (4).
○ Experimental data.

Fig. 4. Strain law for a mild steel at room temperature, according to reference (11)

Calculation of the stress distribution in a cylinder

A method has been worked out for calculating the stress distribution in a thick-walled cylinder subjected to an internal pressure. In this method, which is described in Appendix 1, it is assumed that (*a*) the cylinder is of the closed-end type; (*b*) its length is such that the stress distribution can be considered as independent of the geometry of the heads; and (*c*) it has not yet been subjected to an internal pressure: this restriction is imposed by the fact that equation (2) holds only for a metal which has never been stressed.

It makes use of the law of microplasticity of the material and the strain law proposed above, involving the simple superimposition of plastic shear strains in planes lying at 45° to the principal stresses.

The stress distributions calculated by this method for two cylinders with an r_o/r_n ratio of 2, made from steels C and D respectively, are given in Figs 5 and 6. These two steels were selected because their laws of microplasticity differed greatly. In each case the internal pressure was selected so as to obtain an external circumferential stress of 400 MN/m². Comparison of Figs 5 and 6 shows that:

(*a*) the stress distribution is highly dependent on the law of microplasticity of the material;

(*b*) whatever the case considered, the distinction between elastic and plastic strain loses all significance; and

(*c*) the calculation method can be used over a wide range of laws of microplasticity.

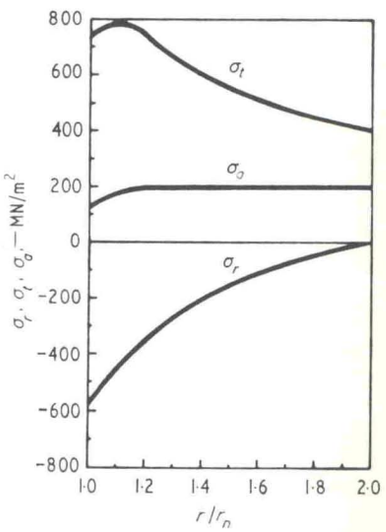

Fig. 5. Stress distribution in a cylinder with an r_o/r_n ratio of 2 made from steel C, subjected to an internal pressure of 5·760 kbar.

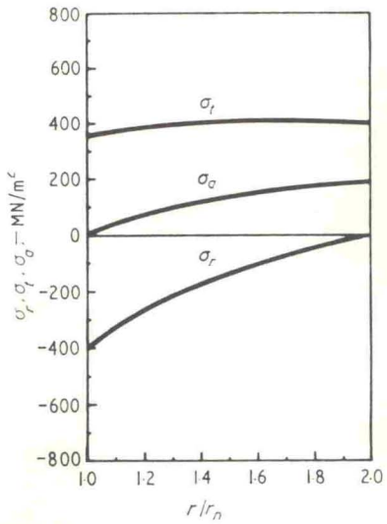

Fig. 6. Stress distribution in a cylinder with an r_o/r_n ratio of 2 made from steel D, subjected to an internal pressure of 3·970 kbar

This calculation method allows the strains at the cylinder's outer radius to be determined. Fig. 7 shows how the following values compare with one another: the microstrains obtained by this calculation, in the case of a cylinder with an r_o/r_n ratio of 2 made from steel D; those derived from the Lévy–von Mises relation; and those measured while the pressure progressively builds up in the cylinder. It is seen that the microstrains calculated according to the proposed method agree closely with the experimental microstrains.

CONCLUSIONS

The results reported above confirm the existence of a size effect in the case of steels A, B, and C: when geometrically similar cylinders made from the same steel are compared, the pressure corresponding to the onset of plastic strain in the cylinder is observed to decrease slightly as the cylinder's size increases. This size effect can be accounted for in terms of Weibull's theory, in which the m exponent increases with increasing yield stress of the material.

A method has been worked out for calculating the stress distribution in a thick-walled cylinder subjected to an internal pressure. This method takes into account the laws of microplasticity of the material and is based on the assumption that plastic strain results from the simple superimposition of plastic shear strains in planes forming

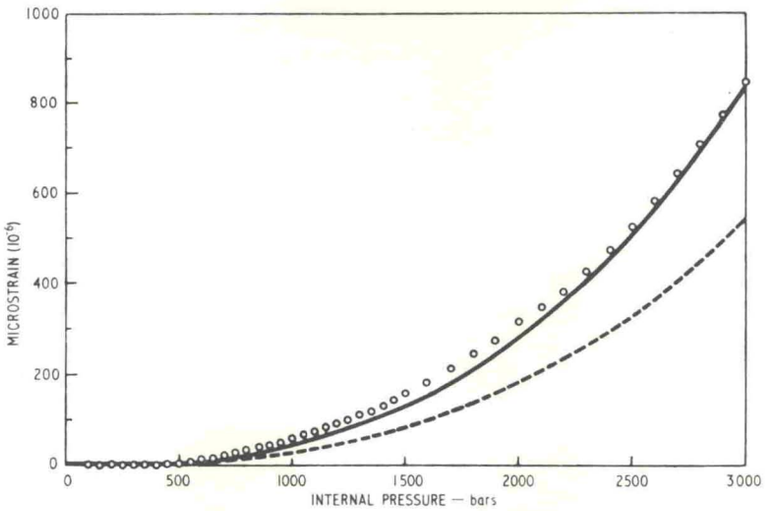

– – – – Calculation based on the Lévy–von Mises strain relation.
——— Calculation based on the new strain law proposed.
○ Experimental data.

Fig. 7. Comparison of the calculated external circumferential strains with those measured on raising the pressure in a cylinder with an r_o/r_n ratio of 2 made from steel D

an angle of 45° with the directions of the principal stresses, each of these strains depending solely on the shear stress in the corresponding plane. Application of this method to two individual cases shows that the stress distribution is highly dependent on the law of microplasticity of the material. The external circumferential strains derived by this method agree closely with those observed experimentally while the pressure builds up in the cylinder.

ACKNOWLEDGEMENTS

The authors wish to thank CRIF (Centre de Recherches Scientifiques et Techniques de l'Industrie des Fabrications Métalliques) and IRSIA (Institut pour l'Encouragement de la Recherche Scientifique dans l'Industrie et l'Agriculture) for supporting the cost of the present work.

APPENDIX 1

Calculation of the stress distribution in a thick-walled cylinder subjected to an internal pressure

A method is proposed for calculating the stress and strain distribution in a long, thick-walled, closed-end cylinder subjected to an internal pressure. For this calculation it will be assumed that the law of microplasticity of the material can be depicted by a relation of the type

$$\epsilon_p = f(\sigma) \quad . \quad . \quad . \quad . \quad . \quad (6)$$

In the case of steel, this relation can take the form of equation (2). For other materials, other relations can be used without calling for any modification of the calculation method. It will further be assumed that the cylinder has never been subjected to an internal pressure. This restriction is related to the fact that equation (2) holds only for a metal which has not been stressed previously.

Based on considerations of symmetry, it will also be assumed that the directions of the principal stresses are known. These principal stresses, σ_r, σ_t, σ_a, are parallel to the radius, the tangent, and the axis of the cylinder, respectively. Due to the symmetry of revolution, these three stresses do not vary with the angle, θ. Furthermore, in the case of a cylinder of sufficient length, σ_r, σ_t, and σ_a can be assumed to be independent of z. Thus, the only variable to be considered is the radius r. It will finally be assumed that a plane section perpendicular to the axis of the cylinder remains plane after deformation: in other words, the total elongation parallel to the axis (ϵ_a) does not depend on r.

Equations to describe the behaviour of material

In the most general case, the ϵ_r, ϵ_t, and ϵ_a strains, which are parallel to the radius, tangent, and axis, comprise an elastic component and a plastic component, though the latter can be nil:

$$\epsilon_t = \epsilon_{te} + \epsilon_{tp} \quad . \quad . \quad . \quad . \quad (7)$$

Two similar equations hold for ϵ_r and ϵ_a. The elastic strains are given by

$$\epsilon_{te} = \frac{1}{E}\left[\sigma_t - \nu(\sigma_a + \sigma_r)\right] \quad . \quad . \quad . \quad (8)$$

and similar equations for ϵ_{re} and ϵ_{ae}, where E is Young's modulus and ν is Poisson's ratio. The microplastic strains are given by three equations of the type

$$\epsilon_{tp} = \tfrac{1}{2}f(\sigma_t - \sigma_a) + \tfrac{1}{2}f(\sigma_t - \sigma_r) \quad . \quad . \quad (9)$$

Method of calculation

The cylinder is divided into n concentric zones of equal thicknesses, the thickness of each zone being small with respect to the wall thickness. Calculation is started from the outer surface of the cylinder and progresses inwards, the zones being numbered $1, 2, \ldots, i, \ldots, n$ in this direction. The principal stresses at the outer radius (r_{i-1}) of the zone, i, viz.

$$\sigma_{r_{i-1}}, \sigma_{t_{i-1}}, \sigma_{a_{i-1}} \quad . \quad . \quad . \quad (10)$$

are known. To calculate the three corresponding stresses at the inner diameter of the same zone, viz.

$$\sigma_{r_i}, \sigma_{t_i}, \sigma_{a_i} \quad . \quad . \quad . \quad . \quad (11)$$

the three following equations are available:

(1) The equation of equilibrium in the radial direction:

$$\frac{d\sigma_r}{dr}+\frac{\sigma_r-\sigma_t}{r}=0 \quad . \quad . \quad . \quad (12)$$

(2) The condition of compatibility:

$$r\frac{d\epsilon_t}{dr}=\epsilon_r-\epsilon_t \quad . \quad . \quad . \quad . \quad (13)$$

(3) The condition which expresses that a plane section perpendicular to the axis remains plane after deformation:

$$\epsilon_{a_i}=\epsilon_{a_o} \quad . \quad . \quad . \quad . \quad (14)$$

where ϵ_{a_o} is the strain parallel to the axis at the outer radius of the cylinder.

Using the system composed of equations (12), (13), and (14) it is possible to derive σ_{r_i}, σ_{t_i}, and σ_{a_i} from $\sigma_{r_{i-1}}$, $\sigma_{t_{i-1}}$, and $\sigma_{a_{i-1}}$. The system is solved by a method of continual approach whose layout is described below.

Starting point of the calculations

The calculations are started at the outer radius of the cylinder, where the boundary conditions impose $\sigma_{r_o}=0$. The two other stresses at the outer radius are selected arbitrarily: σ_{t_o} and σ_{a_o}. The stress field at any point in the cylinder wall can then be calculated by progressing inwards. The boundary condition at the inner radius gives the pressure, p:

$$p=-\sigma_{r_n} \quad . \quad . \quad . \quad . \quad (15)$$

The calculation is thus carried out 'backwards', i.e. the stress distribution is not calculated starting from the internal pressure; on the contrary, the starting point is the stress field at the outer radius, r, and the internal pressure that has to be applied to the cylinder to create this stress field is derived from this starting point.

In actual fact, the problem is not so simple, because σ_{t_o} and σ_{a_o} are not independent variables. If one of these two stresses is chosen arbitrarily, the choice of the other is no longer free. To remove this difficulty use is made of the fact that the internal pressure can be derived, not only from equation (15) but also by equating the force acting on the heads due to the internal pressure with the sum of the axial stresses in a section normal to the axis. The p_a value derived by this means is:

$$p_a=\frac{2}{r_n^2}\int_{r_n}^{r_o}\sigma_a r\,dr \quad . \quad . \quad . \quad (16)$$

The p and p_a values derived respectively from equations (15) and (16) must be equal.

The calculation will thus be carried out by fixing the value of σ_{t_o} and assuming, as a first approximation, that σ_{a_o} has a value $\sigma_{a_o}{}^{I}$, as shown in Fig. 8 which gives the general layout of the calculations. In general, the p and p_a values will not be equal: by comparing these two values, a second approximation of σ_{a_o}, i.e. $\sigma_{a_o}{}^{II}$, can be calculated, the value of σ_{t_o} remaining the same. The calculation is then continued until identical values are obtained for p and p_a.

Calculation of the stresses at the inner radius of a given zone

The stresses at the inner radius of zone i are calculated starting from a first approximation ($\sigma_{r_i}{}^{I}$, $\sigma_{t_i}{}^{I}$, $\sigma_{a_i}{}^{I}$) obtained

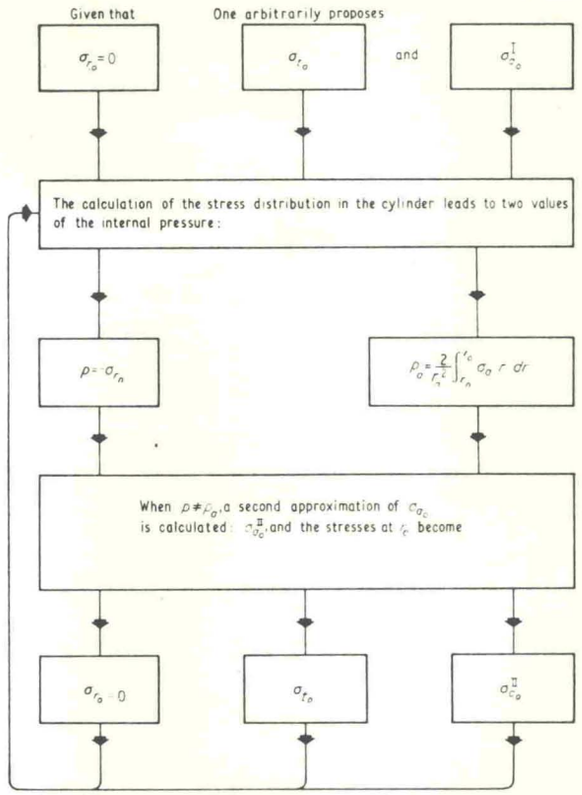

Fig. 8. General layout of calculations

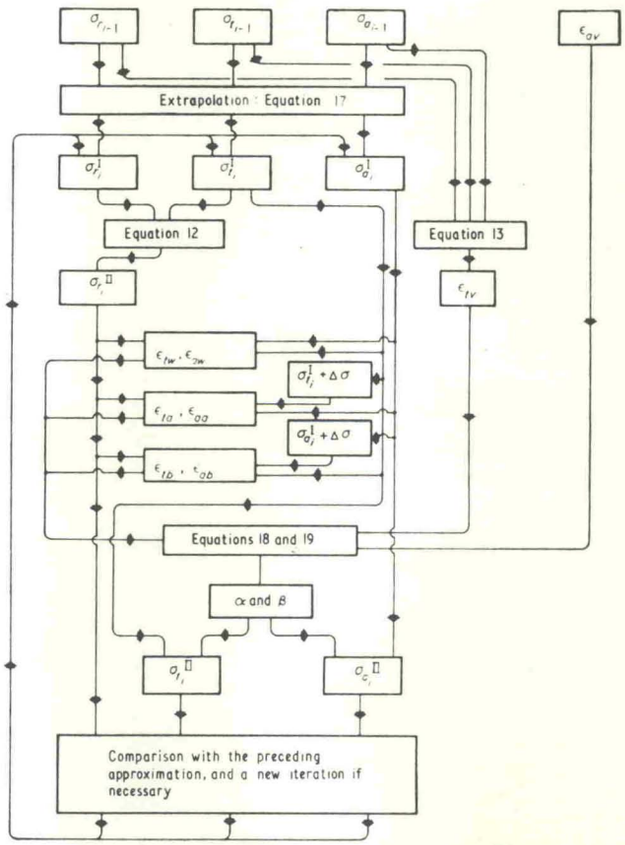

Fig. 9. Layout of a complete iteration

by linearly extrapolating the stress relation for the two preceding zones:

$$\sigma_{r_i}{}^{\mathrm{I}} = 2\sigma_{r_{i-1}} - \sigma_{r_{i-2}} \quad . \quad . \quad . \quad (17)$$

$\sigma_{t_i}{}^{\mathrm{I}}$ and $\sigma_{a_i}{}^{\mathrm{I}}$ being derived from two equations of the same type.

Calculation of the second approximation ($\sigma_{r_i}{}^{\mathrm{II}}$, $\sigma_{t_i}{}^{\mathrm{II}}$, $\sigma_{a_i}{}^{\mathrm{II}}$) is carried out according to Fig. 9, which gives the layout of a complete iteration. The steps in this iteration are as follows:

(1) The second approximation of σ_{r_i} is derived from equation (12).

(2) The value ϵ_{tv}, imposed for the strain ϵ_t by the condition of compatibility, is derived from equation (13); the value ϵ_{av}, imposed for the strain ϵ_a, is given by the stress field at the outer radius and does not depend on the zone considered.

(3) The strains ϵ_{tw} and ϵ_{aw}, corresponding to the stresses $\sigma_{r_i}{}^{\mathrm{II}}$, $\sigma_{t_i}{}^{\mathrm{I}}$, and $\sigma_{a_i}{}^{\mathrm{I}}$, are derived; in most cases these strains are not identical with the strains ϵ_{tv} and ϵ_{av}.

(4) The strains ϵ_{ta}, and ϵ_{aa}, corresponding to the stresses $\sigma_{r_i}{}^{\mathrm{II}}$, $\sigma_{t_i}{}^{\mathrm{I}}+\Delta\sigma$, and $\sigma_{a_i}{}^{\mathrm{I}}$ (where $\Delta\sigma$ is an arbitrary, though relatively small, increment) are derived.

(5) The strains ϵ_{tb}, and ϵ_{ab}, corresponding to the stresses $\sigma_{r_i}{}^{\mathrm{II}}$, $\sigma_{t_i}{}^{\mathrm{I}}$, and $\sigma_{a_i}{}^{\mathrm{I}}+\Delta\sigma$, are derived.

(6) The quantities α and β, defined by the following equations, are derived:

$$\alpha = \frac{(\epsilon_{tv}-\epsilon_{tw})(\epsilon_{ab}-\epsilon_{aw})-(\epsilon_{av}-\epsilon_{aw})(\epsilon_{tb}-\epsilon_{tw})}{(\epsilon_{ta}-\epsilon_{tw})(\epsilon_{ab}-\epsilon_{aw})-(\epsilon_{aa}-\epsilon_{aw})(\epsilon_{tb}-\epsilon_{tw})} \quad (18)$$

$$\beta = \frac{(\epsilon_{av}-\epsilon_{aw})(\epsilon_{ta}-\epsilon_{tw})-(\epsilon_{tv}-\epsilon_{tw})(\epsilon_{aa}-\epsilon_{aw})}{(\epsilon_{ta}-\epsilon_{tw})(\epsilon_{ab}-\epsilon_{aw})-(\epsilon_{aa}-\epsilon_{aw})(\epsilon_{tb}-\epsilon_{tw})} \quad (19)$$

(7) The second approximation of σ_{t_i} and σ_{a_i} is given by

$$\sigma_{t_i}{}^{\mathrm{II}} = \sigma_{t_i}{}^{\mathrm{I}}+\alpha\,\Delta\sigma; \qquad \sigma_{a_i}{}^{\mathrm{II}} = \sigma_{a_i}{}^{\mathrm{I}}+\beta\,\Delta\sigma \quad (20)$$

(8) The second approximation as a whole ($\sigma_{r_i}{}^{\mathrm{II}}$, $\sigma_{t_i}{}^{\mathrm{II}}$, $\sigma_{a_i}{}^{\mathrm{II}}$) is then compared with the first; if they differ, a further iteration is carried out starting from the second approximation, and so on.

Time required for the calculations

The calculation method set out above has been programmed for an IBM 1130 computer. The following example will give an indication of the time required: approximately 6 min were taken to carry out a complete calculation in which the cylinder wall was divided into 200 zones and the three stresses σ_{r_i}, σ_{t_i}, and σ_{a_i}, were printed for 20 points distributed over the thickness of the wall.

APPENDIX 2

REFERENCES

(1) DEFFET, L. and GELBGRAS, J. 'Le comportement des tubes à perois épaisses soumis à des pressions élevées', *Rev. Univ. Mines* (1953) **9**, 725.

(2) DEFFET, L. 'Les travaux de recherche sous pressions élevées', *C. r. XXXI^e Congrès Int. Chimie Ind.* 1959 **1**, 251.

(3) DEFFET, L. and LIALINE, L. 'L'influence de l'épaisseur des tubes sur leur comportement sous pression', *Acta tech., Belg.* 1959 **5**, 1.

(4) DEFFET, L. and GOUZOU, J. 'Study of the deformation and fracture of steel from the examination of the behaviour of thick-walled cylinders submitted to high pressures', Comm. Winter Annual Meeting A.S.M.E., New York 1968 (December).

(5) WEIBULL, W. 'A statistical theory of the strength of materials', *Handl. Ing. Vet. Akad.* 1939, 141.

(6) RICHARDS, C. W. 'Size effect in the tension test of mild steel', *Proc. Am. Soc. Test. Mater.* 1954 **54**, 995.

(7) RICHARDS, C. W. 'Effect of size on the yielding of mild steel beams', *Proc. Am. Soc. Test. Mater.* 1958 **58**, 955.

(8) GOUZOU, J. 'Le problème de la déformation plastique en traction monoaxée dans l'acier doux', Publication C.N.R.M. 1969 (May).

(9) GOUZOU, J., LEROY, V. and HABRAKEN, L. Comm. Colloque Franco-Belge sur les mécanismes de déformation et de rupture dans les matériaux cristallins et amorphes (Université Libre de Bruxelles, Institut des Matériaux, 1967 (December)).

(10) GOUZOU, J. 'Transition des microdéformations aux macrodéformations dans le fer et l'acier doux', *C. r. Acad. Sci.* 1967 **265**, 352.

(11) GOUZOU, J. and MAGNEE, A. 'Critère de plasticité et loi de déformation de l'acier doux', *C. r. Acad. Sci.* 1970 **271C**, 537.

(12) REE, T. and EYRING, H. In *Rheology, theory and application* 1958 vol. III, p. 83 (Academic Press, New York).

(13) LODE, W. 'Versuche über den Einfluss der Mittleren Hauptspannung auf das Fliessen der Metalle Eisen, Kupfer und Nickel', *Z. Phys.* 1926 **36**, 913.